| | | |
|---|---|---|
| ADT | ............. | artificial dead time |
| ASDQ | ............. | Amplifier Shaper Discriminator with charge (Q) |
| ASIC | ............. | application specific integrated circuit |
| BNL | ............. | Brookhaven National Laboratory |
| BSM | ............. | beyond the standard model |
| CBO | ............. | coherent betatron oscillation |
| E821 | ............. | Brookhaven Muon $g-2$ Experiment |
| E989 | ............. | Fermilab Muon $g-2$ Experiment |
| EW | ............. | electroweak |
| FID | ............. | free-induction decay |
| Geane | ............. | Geometry and Error Propagation |
| Geant | ............. | Geometry and Tracking |
| Had | ............. | Hadronic |
| HLbL | ............. | hadronic light-by-light |
| HVP | ............. | hadronic vacuum polarization |
| IBMS | ............. | inflector beam monitoring system |
| LO | ............. | leading order |
| MIP | ............. | minimum-ionizing particle |
| NMR | ............. | nuclear magnetic resonance |
| NLO | ............. | next-to-leading order |
| PMT | ............. | photo-multiplier tube |
| ppb | ............. | parts per billion |
| ppm | ............. | parts per million |
| ppt | ............. | parts per trillion |
| QCD | ............. | quantum chromodynamics |
| QED | ............. | quantum electrodynamics |
| RMS | ............. | root mean square |
| SAM | ............. | Sequential Access via Metadata |
| SDT | ............. | shadow dead time |
| SGT | ............. | shadow gap time |
| SiPM | ............. | silicon photo-multiplier |
| SM | ............. | Standard Model |
| STDP | ............. | short-term double pulse |
| VW | ............. | vertical waist |

# Chapter 1

# Introduction

The prevailing theory of particle physics, the Standard Model (SM), has had tremendous success in describing our universe. It has been used to predict and explain a wide variety of phenomena, particle properties, and interactions to great precision. However, in spite of its success in explaining nearly all experimental results, there remain unanswered questions about our universe. Some of these include the matter-antimatter asymmetry, the source of mass for the neutrinos, the existence of dark matter, and reconciling general relativity and quantum mechanics. Many particle physics experiments around the world are being devised and conducted in order to shed light on these questions and improve our understanding of reality. One such experiment is the Fermilab Muon $g-2$ Experiment (E989), underway at the Fermi National Accelerator Laboratory located in Batavia, Illinois.

This dissertation will describe the E989 experiment and the author's contributions in detail. Chapter 1 will provide experimental and theoretical background to the experiment, as well its motivation. Chapter 2 will describe the experimental principle and specifics of muon production and storage. Chapter 3 will describe the various detector systems. Chapter 4 will describe the straw tracking reconstruction including the track fitting algorithm, as well as some analysis results. Chapter 5 will describe the precession frequency measurement portion of the experiment, and detail analysis results from data taken in the first run of the experiment in 2018. Chapter 6 will conclude the dissertation and the results contained within.

## 1.1 Magnetic moments of particles

All particles have intrinsic properties. One property of charged particles is the magnetic dipole moment.[1] This property of a particle is related to its spin through the equation

$$\vec{\mu} = g\frac{q}{2m}\vec{s}, \tag{1.1}$$

where $\vec{\mu}$ is the magnetic dipole moment of a particle, $\vec{s}$ is its spin vector, $m$ is its mass, $q = \pm e$ where $e$ is the elementary charge, and $g$ is the so called "Landé g-factor". $g$ is a measurable and predictable observable. Since the torque on a particle in a magnetic field $\vec{B}$ is

$$\vec{N} = \vec{\mu} \times \vec{B}, \tag{1.2}$$

the rate at which a particle's spin precesses in a magnetic field will depend on $g$. This is one of the key physics principles in the E989 experiment as will be discussed later.

In a Dirac theory, $g$ is equal to 2 for spin-$\frac{1}{2}$ particles with no internal structure [1]. A simple derivation of this result is given in Reference [2]. However, even for these types of particles, $g$ is not quite equal to 2. Motivated by early experimental measurement discrepancies such as the measurements of the hyperfine structure in hydrogen [3], in 1948 Schwinger calculated the first "radiative correction" to the electron magnetic moment [4]. In the same year Kusch and Foley measured the $g$ factor of the electron to be $g_e = 2.00238 \pm 0.00010$ [5, 6], proving that such radiative corrections were needed in a properly descriptive theory. In a quantum field theory, interactions of the particle with virtual particles in loops will contribute to the value of $g$. In this context, for charged leptons, it is convenient to recast the magnetic dipole moment

[1] *Magnetic dipole moment* and *magnetic moment* are equivalent when talking about particles.

formula as

$$\vec{\mu} = 2(1+a)\frac{q}{2m}\vec{s},$$
$$a = \frac{g-2}{2}, \tag{1.3}$$

where $a$ is called the "magnetic anomaly," and contains all higher order corrections to $g$. The first correction to $a$, calculated by Schwinger, was $a = \alpha/2\pi \approx 0.00116$, where $\alpha$ is the fine structure constant, consistent with the measured value. By measuring $a$, the SM theory can be tested and extensions to it constrained. A precise measurement of the muon magnetic anomaly, or the anomalous magnetic moment of the muon, is the main goal of the Fermilab Muon $g-2$ Experiment.

do you mention $\left(\frac{m_\mu}{m_e}\right)^2$ ?

## 1.2 Standard Model contributions to $a_\mu$

The latest theoretical predictions for the muon magnetic moment will be presented here. The contributions to $a_\mu$ can be divided into three sectors of the SM. These include the quantum-electrodynamics (QED) contributions purely from leptons and photons, the electroweak (EW) contributions from interactions involving the weak force bosons $\{W^\pm, Z^0, H\}$, and the hadronic (Had) contributions from interactions with strongly-interacting hadrons:

$$a_\mu^{\mathrm{SM}} = a_\mu^{\mathrm{QED}} + a_\mu^{\mathrm{EW}} + a_\mu^{\mathrm{Had}}. \tag{1.4}$$

### 1.2.1 QED

The QED contributions to $a_\mu$ stem solely from loops with virtual leptons and photons. They are well understood and have been calculated to sufficient order, having been calculated up to five-loop level from over 13,000 Feynman diagrams [9, 10]. This has been achieved through both analytical and numerical methods. The first couple of diagrams, including the Dirac $g=2$ and Schwinger diagrams, are shown in Figure 1·1.

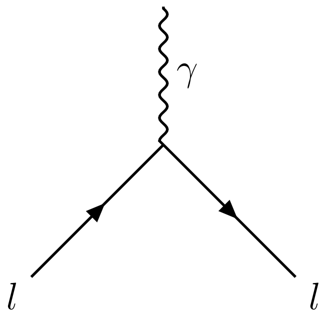


(a) Dirac result, $g = 2$.

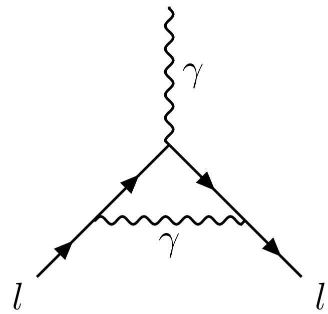


(b) The first loop diagram, calculated by Schwinger.

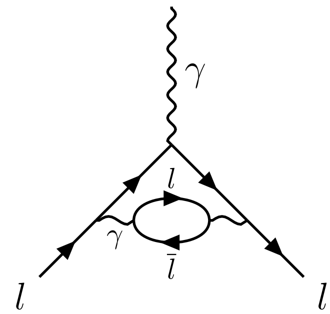


(c) A two-loop diagram.

Figure 1·1: The first of many QED diagrams contributing to $a$. Feynman diagrams made with References [7, 8].

The sum of QED contributions to five-loop level calculated by T. Aoyama et al. is [9, 10]

$$\begin{aligned} a_\mu^{\mathrm{QED}} &= \sum_{n=1}^{\infty} C_n \left(\frac{\alpha}{\pi}\right)^n, \\ &= (11658471.8971 \pm 0.0007) \times 10^{-10}, \end{aligned} \tag{1.5}$$

where in the first line $a_\mu^{\mathrm{QED}}$ is expressed as a perturbative expansion in the fine structure constant, $C_n$ is the coefficient to be determined, and $n$ is the loop level. $C_1 = 1/2$ is the Schwinger result mentioned previously, stemming from the diagram shown in Figure 1·1b. While over 99% of the value of $a_\mu$ comes from the QED sector, the error is much smaller than in the EW and hadronic contributions.

### 1.2.2 Electroweak

The electroweak contributions to $a_\mu$ are known to two-loop level [11]. Estimations of three-loop level contributions and above are small [12]. The different one-loop diagrams are shown in Figure 1·2. In the EW diagrams the heavy masses of the gauge bosons will produce contributions with characteristic scales of of $\sim (m_l/m_{Z^0,H,W^\pm})^2$. Because the masses of the gauge bosons are much larger than the muon, these processes are suppressed and the electroweak contributions to $a_\mu$ are small relative to

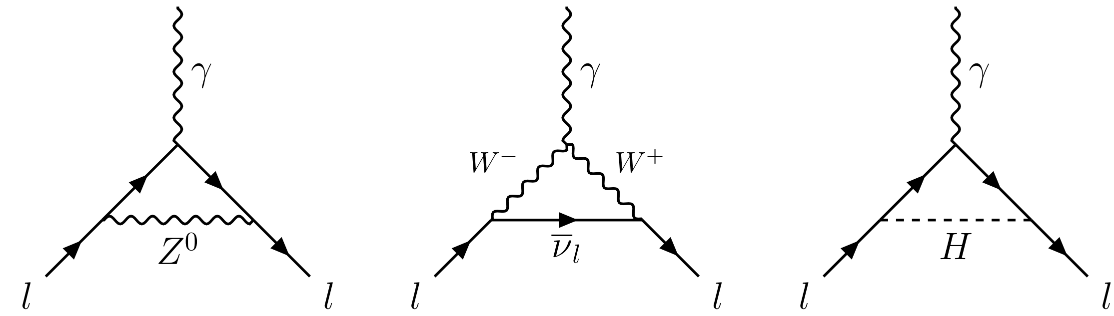


(a) Exchange of a virtual $Z^0$ boson.

(b) Electroweak loop with $W$ bosons.

(c) Exchange of a Higgs boson.

Figure 1·2: First order weak diagrams contributing to $a$. Feynman diagrams made with References [7, 8].

the QED contributions. The value of the electroweak contributions as given by T. Ishikawa et al. is [11]

$$a_\mu^{\text{EW}} = (15.29 \pm 0.10) \times 10^{-10}. \tag{1.6}$$

This value is consistent with the oft-quoted PDG value of $15.36 \pm 0.10 \times 10^{-10}$ [12]. It should be noted that the error on these contributions is small compared to those of the hadronic contributions discussed next.

### 1.2.3 Hadronic

The hadronic contributions to $a_\mu$ arise from loop diagrams with virtual hadrons. Because the strong coupling is large at low energies, the amplitudes for these processes cannot be calculated perturbatively. As the low-energy non-perturbative processes dominate the hadronic contributions, they by extension have errors that dominate the theoretical uncertainty in the SM calculation. Most active work on $a_\mu$ in the theoretical community is in this sector. The Muon $g-2$ Theory Initiative is comprised of many working groups from various institutions which seeks to make improvements in the hadronic calculations, and produce consensus values going forward in 2020 and beyond [13]. The hadronic contributions can be separated into two parts:

$$a_\mu^{\text{Had}} = a_\mu^{\text{HVP}} + a_\mu^{\text{HLbL}}. \tag{1.7}$$

**Hadronic Vacuum Polarization**

The first term in Equation 1.7 refers to contributions from hadronic vacuum polarization (HVP), the first order diagram of which is shown in Figure 1·3a. There are two main prescriptions for calculating these contributions. The first is to use a dispersive approach to introduce a virtual hadron bubble into the integral calculation for the photon propagator[2], and then utilize the optical theorem to relate the imaginary part of that propagator to the total cross-section of electron-positron annihilation to hadrons [15]. While this could be solved perturbatively for a lepton bubble in place of the hadron bubble, this is instead a data driven approach when considering non-perturbative QCD. The leading order (LO) contribution can be written as

$$a_\mu^{\text{HVP;LO}} = \left(\frac{\alpha m_\mu}{3\pi}\right)^2 \int_{m_\pi^2}^{\infty} \frac{ds}{s^2} K(s) R(s), \tag{1.8}$$

where $K(s)$ is some calculable kinematic factor, and $R(s)$ is a ratio of cross-sections,

$$R(s) = \frac{\sigma(e^+e^- \to \text{hadrons})}{\sigma(e^+e^- \to \mu^+\mu^-)}. \tag{1.9}$$

The cross-section data for Equation 1.9 has been measured in different energy ranges by various experiments; a brief overview is given by A. Keshavarzi et al. [16]. There are two approaches to measuring this cross-section data. The first operates at fixed center of mass energies in the standard collider theme, and the second tags initial state radiation in order to evaluate the differential cross-section over a wider energy range. As further data ~~is~~ are acquired and compared between the different experiments,

[2] The details of dispersion theory will not be described here but a pedagogical introduction is given in Reference [14].

I don't think you need to cite this package but it's OK to do so.



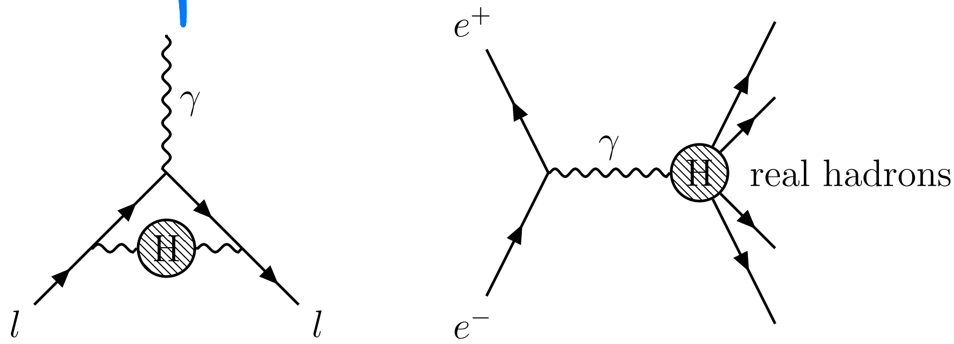


(a) The first order HVP Feynman diagram.

(b) The Feynman diagram for electron positron annihilation to hadrons.

Figure 1·3: The first order HVP diagram on the left, which can be related to the diagram on the right via the optical theorem. The H bubble in both diagrams indicates all hadrons. Feynman diagrams made ~~with References~~ [7, 8].

using TikZ-Feynman [7, 8]

the error in the HVP contributions to $a_\mu$ will decrease. The analysis by Keshavarzi et al. with cross-section data as of November 1st, 2019 gives results as [17, 18]

$$\begin{aligned} a_\mu^{\mathrm{HVP;LO}} &= (692.78 \pm 2.42) \times 10^{-10}, \\ a_\mu^{\mathrm{HVP;NLO}} &= (-9.83 \pm 0.04) \times 10^{-10}, \end{aligned} \tag{1.10}$$

where $a_\mu^{\mathrm{HVP;NLO}}$ is the next-to-leading (NLO) order calculation. This evaluation is consistent with another more conservative analysis by Davier et al. [19, 20]. A calculation for the next-to-next-to-leading order HVP contribution is given by A. Kurz et al. [21]

$$a_\mu^{\mathrm{HVP;NNLO}} = (1.24 \pm 0.01) \times 10^{-10}. \tag{1.11}$$

The second prescription for estimating the HVP contributions is a first principles approach, using lattice QCD. Lattice QFT is a gauge theory defined on a finite ensemble of discretized points in time and space. In the limit that the ensemble is taken infinitely large with the spacing between the points infinitesimally small, the behavior from a continuous theory is recovered. The lattice-based estimates of

$a_\mu^{\mathrm{HVP;LO}}$ are consistent with those provided above, though the error is larger [22].

### Hadronic Light-by-Light

The second of these hadronic contribution parts is a higher-order, four-photon interaction, termed hadronic light-by-light (HLbL). Diagrams are shown in Figure 1·4. The calculation of these diagrams has historically been model dependent, and has therefore been the most contentious part of the SM calculation. The value of the HLbL contributions to $a_\mu$ from model estimates by the so-called ‘Glasgow consensus’ is $a_\mu^{\mathrm{HLbL}} = (10.5 \pm 2.6) \times 10^{-10}$ [23].

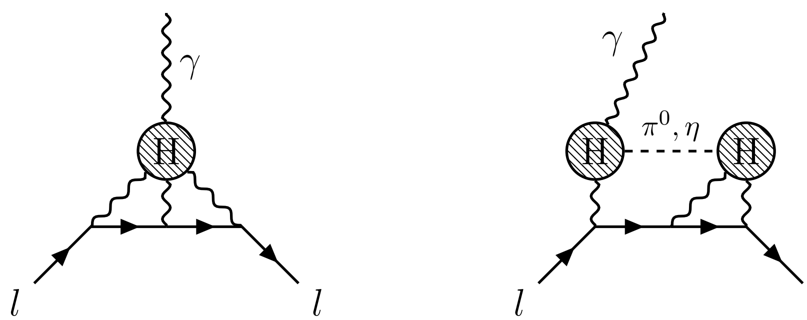


Figure 1·4: HLbL diagrams contributing to $a_\mu$, where three photons are exchanged with a virtual hadrons bubble. The diagram on the right is technically contained within the diagram on the left, however it is displayed separately here in order to help illustrate the complexity of this contribution. Feynman diagrams made with References [7, 8].

In more recent years, there have been efforts to produce results using dispersive [24, 25, 26, 27, 28, 29, 30, 31] and lattice approaches [32, 33]. A calculation of the HLbL contribution using the sum of the dispersive results with linearly added errors given by ~~A.~~ Keshavarzi et al. from the references listed above is [18][3]

no A

$$a_\mu^{\mathrm{HLbL}} = (9.34 \pm 2.92) \times 10^{-10}. \tag{1.12}$$

[3]Some pieces are still from the Glasgow consensus which are a work in progress. These dominate the error in the HLbL contribution.

This calculation, while consistent with the Glasgow consensus estimate provided above, has the advantage that it is in part model-independent. The error on this contribution is relatively large in each of these various approaches, comparable to that of the $a_\mu^{\mathrm{HVP;LO}}$ term, even though the size of this contribution is small. A calculation of the higher order HLbL contributions by Colangelo et al. gives [34]

$$a_\mu^{\mathrm{HLbL;NLO}} = (0.30 \pm 0.20) \times 10^{-10}, \tag{1.13}$$

showing that higher order HLbL contributions are practically negligible.

### 1.2.4 Combined Standard Model value

The sum of the $a_\mu$ contributions listed here is [9, 10, 11, 18, 21, 23, 34]

$$\begin{aligned} a_\mu^{\mathrm{SM}} &= a_\mu^{\mathrm{QED}} + a_\mu^{\mathrm{EW}} + a_\mu^{\mathrm{Had}}, \\ &= (11659181.02 \pm 3.80) \times 10^{-10}. \end{aligned} \tag{1.14}$$

The relative uncertainty of this result is 326 parts per billion (ppb). Other analyses with different values for the various contributions typically agree well, as shown on the left side of Figure 1·5. In general, the consistency of the theory has been stable for almost ten years now. Depending on which calculations are used, the discrepancy between theory and experiment ranges between 3 to 4 standard deviations.

## 1.3 Experimental value of $a_\mu$ and discrepancy with $a_\mu^{\mathrm{SM}}$

have

The theoretical contributions to $a_\mu$ listed in the previous sections ~~have~~ improved over time as methods have matured and more experimental data has been gathered. Similarly, work on the direct experimental measurement of $a_\mu$ has been going on for decades, with more precise results being determined over time [35]. The most recent experiment to measure $g - 2$ was the Brookhaven Muon $g - 2$ Experiment (E821) you should acknowledge that the Fig came from the reference,



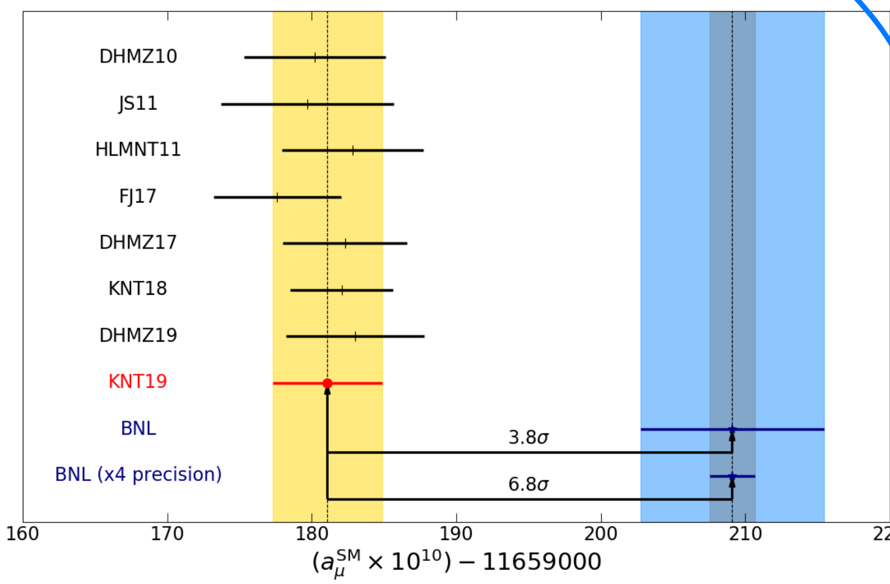


Figure 1·5: Various theoretical values for $a_\mu$ on the left, as compared to the most recent and future extrapolated experimental results on the right [18].

From Ref. [18]

held at Brookhaven National Laboratory (BNL), which collected data from 1997 to 2001. That experiment measured a value for $a_\mu$ of [36, 37]

$$a_\mu^{\text{Exp}} = (11659208.9 \pm 6.3) \times 10^{-10}, \tag{1.15}$$

which corresponds to a 540 ppb relative uncertainty. Note that the uncertainty of the experimental measurement is comparable to that of the theory, necessitating a precise understanding of all the different theoretical parts. The difference between the experimental and theoretical values presented here is

what does this mean?

$$a_\mu^{\text{Exp}} - a_\mu^{\text{SM}} = (27.88 \pm 7.36) \times 10^{-10}, \tag{1.16}$$

corresponding to a discrepancy of 3.79 standard deviations.

to resolve "the two" what?
do you mean the difference?



## 1.4 Beyond the Standard Model and the purpose of E989

While the discrepancy between experiment and theory might be attributed to miscalculations in the theory or systematic errors in the E821 experiment (or a very rare statistical fluctuation), no such errors have been found despite repeated attempts to resolve the two. Indeed the discrepancy has only grown over time as the theoretical calculations have matured. The most intriguing and exciting source of the discrepancy would be physics beyond the standard model (BSM).

The value of $a_\mu$ receives contributions from all particles that couple to the muon through virtual loops, so it is possible that unknown particles are the source of this discrepancy. The contribution to the magnetic moment from heavy virtual particles goes as

"as yet undiscovered"?

$$a \sim C\frac{m^2}{\Lambda^2}, \tag{1.17}$$

where $C$ is a constant of $\mathcal{O}(1)$, $\Lambda$ is the mass scale of the new physics, and $m$ the mass of the lepton in question. The postulation of such new heavy particles has long been explored in supersymmetry models [38]. However, with the lack of positive results coming out of the LHC experiments, such models are mostly excluded barring some parameter space [39]. Radiative mass mechanisms in the range of $1-2$ TeV could be the source of the discrepancy while also accounting for the small muon mass relative to the electroweak gauge bosons [38]. Heavy scalar leptoquarks, two-Higgs-doublet, or more general scalar doublet models can also be constructed which account for the discrepancy [40, 41, 42].

What does this mean?

The sensitivity of the muon as compared to the electron to large mass scales is $m_\mu^2/m_e^2 \approx 43,000$ times greater. For this reason, it is possible that even though the g-factor of the electron has been measured extraordinarily precisely, to 0.26 parts per trillion (ppt) corresponding to a 0.23 ppb relative uncertainty in $a_e$ [37, 43],

they measure $a_e$ but quote $g_e$ to make their measurement sound more impressive.

it has not yielded a definitive difference between theory and experiment, whereas the magnetic moment of the muon might do so. With that being said a recent measurement of the fine structure constant $\alpha$ to the highest precision yet [44] has yielded a new value of $a_e$ for which the difference between theory and experiment is 2.5 standard deviations, but with the opposite sign as compared to $a_\mu$. To explain both discrepancies simultaneously implies that the electron and muon sectors need to be decoupled from one another in light of the constraints from $\mu \to e\gamma$. Models with vector-like fermions which can account for both discrepancies can be formulated whereas other models have trouble [45].

BSM models at the low energy regime can also explain the discrepancy. These include a light scalar 'dark' Higgs which may be capable of producing the discrepancy [46], (regardless of the fact that the dark photon model has been ruled out at the 99% confidence level [47]), and low mass pseudo-scalar axion-like particles [48], among others.

Fermilab

Future data taken from the LHC and other experiments will further constrain the possible models based on other experimental observables. The E989 experiment was undertaken in order to improve the experimental precision of the $a_\mu$ measurement, while verifying the previous result. Although, in general, there has been a lack of new physics results from other experiments, E989 has the potential to provide an indirect confirmation of new physics. Accordingly, interest in the E821 experiment and it's successor E989 has grown over time. The number of citations for the E821 results has been consistently high for 20 years as shown in Figure 1·6.

The E989 experiment has the goal of measuring $a_\mu$ to 140 ppb by 2021. This would be a factor of four improvement over the E821 result stemming from a twenty times increase in statistics, which was the dominant error in the previous experiment. Assuming the same central value for $a_\mu$ is obtained, this new measurement would push the statistical

I will suggest an alternate way to say this.

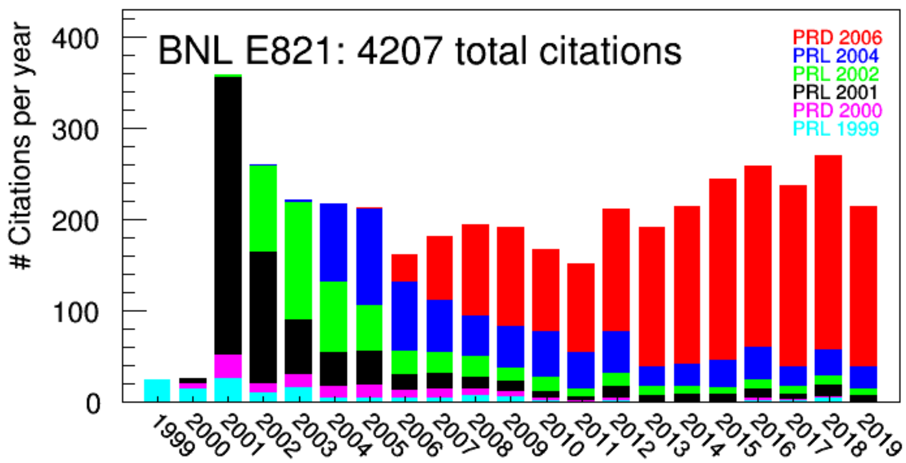


Figure 1·6: The number of citations for the BNL experiment E821 publications as a function of year, as of 10/30/2019 [49].

significance of the discrepancy to approximately seven standard deviations, as shown in Figure 1·5. The data comprising Run 1, gathered between April and July of 2018, is the subject of this thesis, and corresponds to a statistical uncertainty comparable to the E821 result. The Run 1 result by itself may ~~give~~ strong evidence for new physics, depending on the new measured value for $a_\mu$. provide